Nanotubes

DOI: 10.1002/ange.201102976

Formation of Efficient Catalytic Silver Nanoparticles on Carbon Nanotubes by Adenine Functionalization**

Prabhpreet Singh, Giuseppe Lamanna, Cécilia Ménard-Moyon, Francesca Maria Toma, Elena Magnano, Federica Bondino, Maurizio Prato, Sandeep Verma, and Alberto Bianco**

Carbon nanotubes (CNTs) are currently receiving enormous attention as advanced nanomaterials, mainly because of their conductive, thermal, mechanical, and chemical properties.[1] CNTs can be employed in composites, transistors, or sophisticated electrodes, to mention just a few applications.[2,3] In addition, because of their nanoscale dimensions and high aspect ratio, CNTs have a huge surface area, which may be exploited to achieve efficient catalytic processes.[4,5] However, the difficult handling and the lack of complete control over the CNTs inhibit their use on a large scale. In this respect, extraordinary progress has been achieved in the field of chemical functionalization of CNTs.[6,7] The modification of the CNT surface by using a wide variety of chemical approaches, and the combination of the different physicochemical properties have allowed the fast development of CNTs as a support for growing catalytic metal nanoparticles.[8–10]

As catalysis represents a fundamental tool for improving the efficiency of many processes, the design of novel building blocks and nanoparticles will contribute to the development of advanced catalysts.[11,12] In particular, solid catalysts endowed with a high surface area allow high efficiency of catalyzed chemical reactions.[13] To prepare metal nanoparticle/CNT hybrids, several approaches have been explored,[14] including the reduction of metal salts,[15,16] the spontaneous reduction of gold and platinum nanoparticles on nanotubes,[17,18] an electrochemical route to reduce metal ions,[19,20] a chemical deposition method,[21] and the thermal decomposition of metal salts.[22,23] Recently, N-doped multiwalled CNTs (MWCNTs) have been used to anchor silver nanoparticles.[24] However, appropriate CNT functionalization to tailor catalytic molecule deposition has not yet been explored, though it can become an attractive tool.

Herein, we describe a simple methodology to template the growth of silver nanoparticles (NPs) on the surface of MWCNTs, and the use of the resulting hybrids as catalyst for the oxidation reaction of 2-methylhydroquinone to 2-methylbenzoquinone. Benzoquinones are an important class of molecules with antioxidant, anti-inflammatory, and anticancer activities.[25] We have chosen the transformation of hydroquinones as a model reaction to prove the efficiency of the new CNT/NP hybrids. Indeed, heterogeneous catalysis to produce quinones with high recovery yield and recycling efficiency has not been extensively explored. We demonstrate that it is possible to tailor the coordination of Ag NPs onto a MWCNT surface by covalent functionalization of oxidized MWCNTs with a modified adenine moiety. Indeed, the presence of the adenine functional groups on MWCNTs induces the formation of Ag NPs through metal/adenine coordination. MWCNT/Ag complexes are efficient and reusable heterogeneous catalysts for the oxidation of hydroquinones.

In the process of designing new CNT/NP hybrids, we focused our attention on using functional groups that favor the growth of NPs directly at the surface of functionalized CNTs. Adenine, a purine nucleobase, is endowed with suitable metal ion binding sites. Indeed, the exocyclic amino group at C6 and the four imino groups at the N1, N3, N7, and N9 positions have been exploited to build interesting supramolecular structures as well as to support metal-assisted catalytic transformations.[26] Based on these characteristics of adenine, we covalently functionalized MWCNTs with the nucleobase to decorate the surface of the nanotubes with silver nanoparticles. We generated three different types of functionalized CNTs from oxidized MWCNTs (ox-MWCNT; Figure 1 A) to probe the key role played by adenine. Adenine-MWCNTs (Ad-MWCNT) **1a** were prepared by activation of ox-MWCNT by forming the corresponding acyl chloride, and subsequent reaction with a monoprotected diaminotriethylene glycol (TEG) spacer. After deprotection, 3-(9-adeni-

[*] Dr. P. Singh,[+] Dr. G. Lamanna,[+] Dr. C. Ménard-Moyon, Dr. A. Bianco
CNRS, Institut de Biologie Moléculaire et Cellulaire
Laboratoire d'Immunologie et Chimie Thérapeutiques
67000 Strasbourg (France)
E-mail: a.bianco@ibmc-cnrs.unistra.fr
Dr. F. M. Toma, Prof. M. Prato
Dipartimento di Scienze Farmaceutiche, Università di Trieste
34127 Trieste (Italy)
Dr. E. Magnano, Dr. F. Bondino
IOM CNR, Laboratorio TASC
34149 Trieste (Italy)
Prof. S. Verma
Department of Chemistry, Indian Institute of Technology-Kanpur
Kanpur-208016 UP (India)
E-mail: sverma@iitk.ac.in
[+] These authors contributed equally to this work.

[**] This work was supported by the French-Indian CEFIPRA/IFCPAR collaborative project (project no. 3705-2). P.S. wishes to thank CEFIPRA/IFCPAR for a postdoctoral fellowship. TEM images were recorded at the RIO Microscopy Facility Platform of Esplanade Campus (Strasbourg, France). HRTEM and ED were recorded at the IPCMS facility in Cronenbourg (France). We wish to thank Dris Ihiawakrim for helpful discussions, and Loredana Casalis and Pietro Parisse for help on the preparation of XPS samples. G.L. wishes to thank the European Union (ANTICARB program: HEALTH-2007-201587) for financial support.

Supporting information for this article is available on the WWW under http://dx.doi.org/10.1002/anie.201102976.

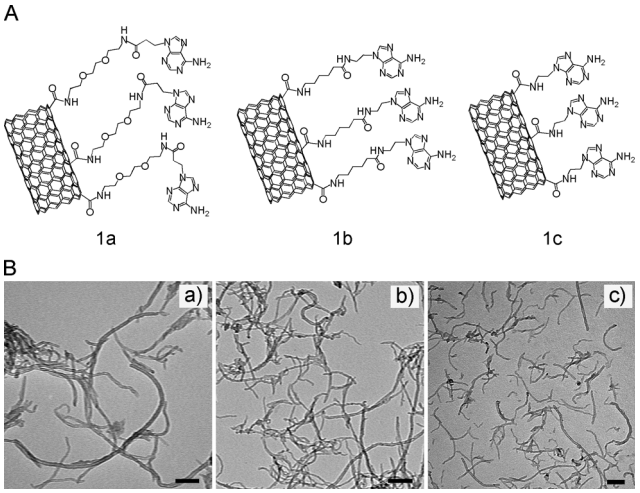

Figure 1. Chemical structures and TEM characterization of the different adenine-functionalized carbon nanotubes. A) The three Ad-MWCNTs **1a**, **1b**, and **1c** contain different spacers between the tubes and the adenine moiety. B) TEM images of Ad-MWCNTs a) **1a**, b) **1b**, and c) **1c** allow observation of the morphology of the different Ad-MWCNTs. Scale bars = 100 nm.

nyl)propionic acid was coupled to the nanotubes. Similarly, Ad-MWCNTs **1b** and **1c** were prepared by the same activation reaction of ox-MWCNT and functionalization with 6-amino-*N*-(2-(6-amino-9*H*-purin-9-yl)ethyl)hexanamide and 9-(2-aminoethyl)adenine, respectively (see the Supporting Information). These three derivatives contain spacers that, in principle, may modulate the solubility in different solvents (i.e., hydrophilic triethylene glycol versus hydrophobic hexanoic linker). In addition, by changing the distance of adenine from the CNT surface, electron transfer and catalytic processes could be accurately controlled. In this context, the deposition of Ag NPs onto the surface of CNTs was achieved by simply mixing a methanolic solution of $AgNO_3$ to the three different Ad-MWCNTs, so that Ag NPs spontaneously grew on the nanotube surface.

The degree of functionalization of the oxidized MWCNTs and the adenine-modified conjugates (**1a**, **1b**, and **1c**) were initially evaluated by thermogravimetric analysis (TGA) under a N_2 atmosphere (see Figure S2 in the Supporting Information). The TGA curves of Ad-MWCNTs **1a**, **1b**, and **1c** show a weight loss of about 23.0%, 21.7%, and 20.0% at 500 °C, respectively, as compared to 11.7% for ox-MWCNT. On this basis, we estimated that the amount of functional groups per gram (f_w) of Ad-MWCNTs **1a**, **1b**, and **1c** was 0.33, 0.34, and 0.48 mmol g^{-1}, respectively, which correspond to one adenine molecule every 222, 220, and 164 carbon atoms, respectively.

The functionalized CNTs were then characterized by transmission electron microscopy (TEM). The TEM images of Ad-MWCNTs **1a**, **1b**, and **1c** show rather isolated nanotubes with the presence of very small aggregates when deposited from dispersions in 1:1 methanol/H_2O (Figure 1B). The CNTs appear debundled, thus confirming the important role of adenine on the modulation of the dispersibility properties of CNTs (for comparison, see the TEM image of ox-MWCNT in Figure S4 in the Supporting Information).

MWCNT/Ag nanohybrids were also analyzed by TEM (Figure 2A). We observed a homogenous distribution of Ag NPs over the surface of the nanotubes. An average size of

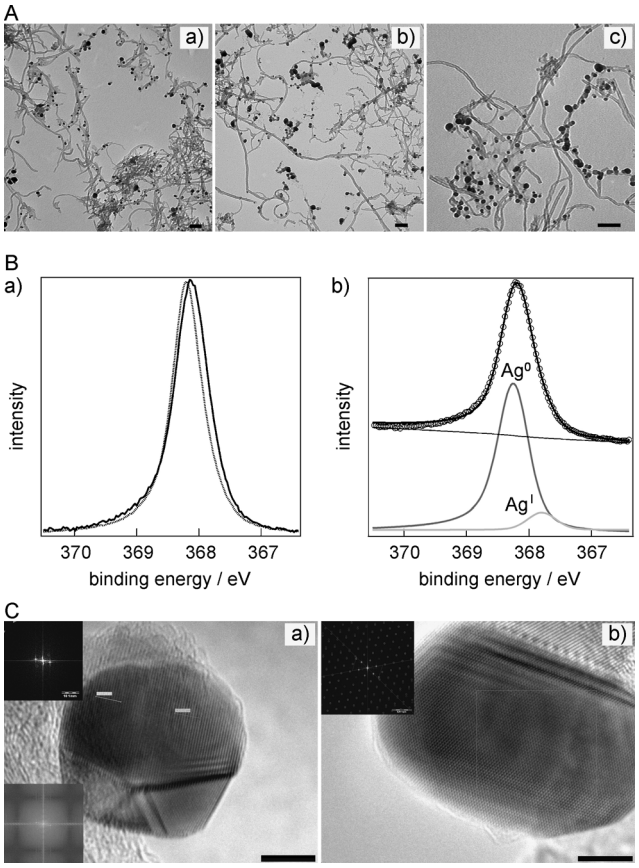

Figure 2. Characterization of the silver/CNT nanohybrids. A) TEM images of Ad-MWCNT hybrids a) **1a**, b) **1b**, and c) **1c** complexed with Ag NPs. Scale bars = 100 nm. B) Ag $3d_{5/2}$ XPS spectra. a) Ad-MWCNT **1a** (black line) and metallic silver (dark-gray line). The integrated background was subtracted and the two spectra were normalized to their maximum intensity. b) Ad-MWCNT **1a** (black circles). The results of the fitting procedure are reported in solid lines. The best fit of this spectrum was obtained by using two components, a main component (dark-gray line) centered at 368.2 eV BE (Gaussian width = 0.4 eV, Lorentzian width = 0.27 eV, asymmetry = 0.067) and a second component (light-gray line) shifted 0.4 eV toward a lower binding energy (Gaussian width = 0.4 eV, Lorentzian width = 0.27 eV, asymmetry = 0). C) HRTEM and ED patterns of a) Ag^0 and b) Ag_2O NPs on Ad-MWCNT **1a** and corresponding fast Fourier transformations. Scale bars = 5 nm.

about (22.6 ± 0.5) nm (mean ± SEM, $n = 325$) could be calculated from the statistical analysis of the NPs on Ad-MWCNT **1a** (see Figure S3 in the Supporting Information). Similar dimensions were also found when the other adenine-modified nanotubes **1b** and **1c** were used, thus demonstrating that the spacer between the tubes and the nucleobase does not influence the NP diameter. In a control experiment, after mixing the $AgNO_3$ solution with ox-MWCNT, TEM images

showed only physical adsorption of big clusters of silver on the bundles of nanotubes (see Figure S4 in the Supporting Information).[27]

We analyzed the composition of these Ag NPs by using a combination of energy dispersive X-ray (EDX), X-ray photoelectron spectroscopy (XPS), and electron diffraction (ED) techniques. The EDX spectrum of NPs clearly shows the peak that corresponds to silver (see Figure S5 in the Supporting Information). The analysis of several particles also allowed us to observe the presence of peaks associated with oxygen. EDX provides information about the chemical composition of a sample, and only confirmed the presence of silver without the possibility to assess its valence. Therefore, we extended the characterization by using XPS in order to evaluate the different oxidation states of silver. Ag $3d_{5/2}$ spectra measured on a clean polycrystalline silver foil and on Ad-MWCNT **1a** are shown in Figure 2B (left-hand panel). For a better comparison, an integrated background was subtracted and the two spectra were normalized to their maximum intensity. An evident energy shift of the Ad-MWCNT **1a**/Ag $3d_{5/2}$ core level toward a lower binding energy (BE) with respect to the BE of metallic silver (368.2 eV), and a broadening of the peak were observed. A fit procedure of the Ag $3d_{5/2}$ spectra (Figure 2B, right-hand panel), carried out by using a Doniach–Sunjic line shape convoluted with a Gaussian function, shows the simultaneous presence of two states of silver oxidation, at BE values of (368.2 ± 0.1) eV and (367.8 ± 0.1) eV, which are ascribed to Ag^0 and Ag^I, respectively. The energy position of the first component corresponds to that of the measured silver foil and shows an asymmetric line shape typical of a metallic system. The assignment of the second component to Ag^I ions is in agreement with the reported data.[28] From this analysis, Ag^0 represents the main contribution to the Ag $3d_{5/2}$ peak, a result that is consistent with the results obtained by using ED (see below). By measuring an XPS spectrum in a wide BE range (see Figures S6 and S7 in the Supporting Information), a quantitative estimate of the total amount of silver at the surface probing depth of around 1.5 nm could be obtained;[29] the amount of silver was about 1.3% of the amount of carbon. However, we have to point out that this value is an underestimation of the total amount of Ag NPs as assessed by TGA (see below).

Finally, to have a complete overview of the NP characterization, we used high-resolution TEM (HRTEM) coupled with ED on selected areas to elucidate the structure of the silver NPs complexed to Ad-MWCNT **1a** at atomic resolution. We analyzed several NPs and found that most of them have preferentially aligned crystalline planes. Figure 2C shows a representative HRTEM image and the corresponding ED patterns of two Ag NPs, and gives information on their phase structure. In accordance with XPS, we found that most of the NPs were constituted of Ag^0. Figure 2C(a) indicates that the NP is constituted of Ag^0 with a face-centered cubic structure and an interplane distance of 2.37 Å, thus corresponding to the most intense plane (111). This result is not surprising as the conditions to generate the NPs allow the reduction of Ag^I to Ag^0.[30,31] However, we also observed silver oxide NPs. The electron diffraction pattern shown in Figure 2C(b) is consistent with hexagonal Ag_2O with mesh parameters of 3.08 Å and 4.94 Å. The most intense electron diffraction ring corresponds to the plane (101) with a spacing of 2.33 Å. Within the different NPs analyzed, we could see a few silver oxide NPs composed of Ag^{II} and some amorphous particles. From the detailed analysis of the HRTEM micrographs and electron diffraction we can conclude that most of the nanoparticles complexed to Ad-MWCNT **1a** were crystalline. The oxidation state of silver is variable as the nanoparticles are either silver metal, silver(I) oxide, or silver(II) oxide, with the majority of the NPs composed of silver metal.

To evaluate the potential of these new silver NPs coordinated to CNTs in heterogeneous catalysis, we investigated the catalytic activity of the Ag NPs in the oxidative reaction of hydroquinones to benzoquinones (Figure 3A).

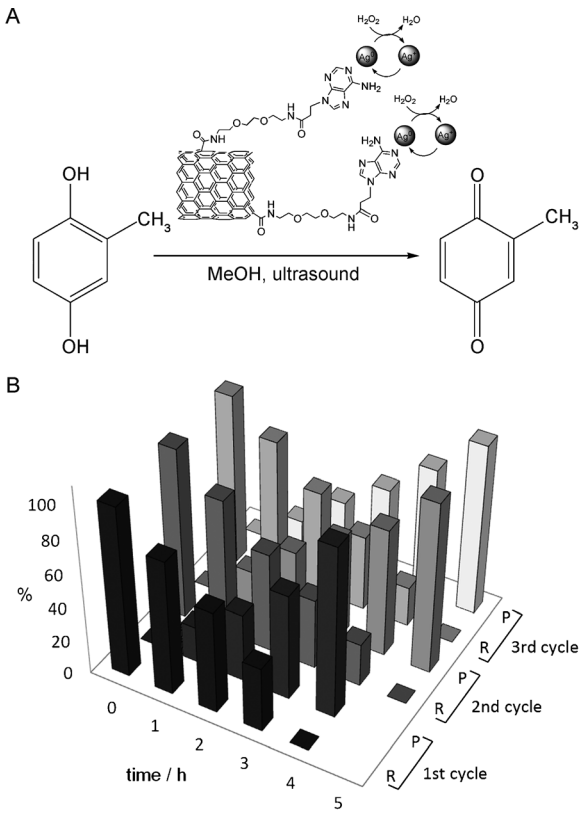

Figure 3. Catalytic reaction using silver/CNT nanohybrids. A) Oxidation reaction of 2-methylhydroquinone to 2-methylbenzoquinone by Ag NPs complexed to Ad-MWCNT **1a** in the presence of hydrogen peroxide under sonication. B) Percentages of conversion following three cycles. R = reagent; P = product.

This reaction was selected as a model for testing the MWCNT/Ag hybrids. Quinones can be obtained by using various oxidants, but most of these reagents produce large amounts of harmful waste, while others are not practical for large-scale preparation because of their high cost.[25,32] The development of recyclable solid-supported catalysts with low environmental impact is becoming highly important.[33,34]

As a proof-of-concept, we explored the catalytic activity of silver NPs complexed to Ad-MWCNT **1a** on the oxidation

of 2-methylhydroquinone to 2-methylbenzoquinone. We initially assessed the amount of Ag NPs on the nanohybrids by using TGA in air. We measured a quantity of Ag NPs that corresponded to 3% of the total amount of the nanohybrids (see Figure S10 in the Supporting Information). This value was used for the calculation of the amount of NPs added to the catalytic reaction. To obtain the reference product, we began with the oxidation of 2-methylhydroquinone in methanol with 35% aqueous H_2O_2 in the presence of commercially available Ag_2O NPs, as previously reported.[35] The evolution of the model reagent 2-methylhydroquinone to 2-methylbenzoquinone could be easily followed by HPLC analysis. Since most of the NPs on the nanotubes were constituted of metallic silver, we also evaluated the efficacy of commercially available Ag^0 NPs of sizes below 100 nm. Indeed, both silver oxide and metallic silver catalyzed the transformation of the hydroquinone, although not to completion (see the Supporting Information).

These control experiments allowed to rationalize the heterogeneous catalytic reaction with our MWCNT/Ag NP hybrids. The oxidation of 2-methylhydroquinone was carried out in methanol in the presence of 35% aqueous H_2O_2 and 0.03 equivalents of NPs on Ad-MWCNT **1a**. The resulting reaction mixture was sonicated at room temperature to maintain a good dispersion of the nanotubes at all stages of the catalytic cycle. After 4 h, we observed the complete disappearance of the starting material and the formation of the desired 2-methylbenzoquinone (see Figure 3B, and Figure S11 in the Supporting Information). The catalytic oxidation was completely selective, as we did not observe the production of any substituted biaryl because of the competitive oxidative homocoupling of 2-methylhydroquinone.[35,36] At the end of the reaction, we easily recovered the nanotubes by simple centrifugation and without any further purification. The collected hybrids were reused under the same reaction conditions for two additional cycles to give similar excellent conversion (Figure 3B). After the third cycle, the NPs were still present as assessed by TEM (data not shown). We also confirmed the oxidation state of Ag NPs after the three catalytic cycles by using XPS. We did not observe significant variations on the composition of the nanoparticles (see Figure S12 in the Supporting Information). In addition, as an alternative control to assess the key role of adenine as a ligand for the NP coordination, we prepared a hybrid by using the nanotubes with only the ammonium groups (f-MWCNT **9**, precursors of Ad-MWCNT **1a**; see Scheme S2 in the Supporting Information). In this case, we could generate Ag NPs on CNTs with a wider diameter distribution (see Figure S13 in the Supporting Information). We then tested the catalytic capacity of this complex on the oxidation of 2-methylhydroquinone without obtaining the desired product (see Figure S14 in the Supporting Information). After obtaining this result, we observed the complex by TEM (results not shown), and surprisingly, we did not find any NP on the grid, thus confirming the important role of adenine in comparison to primary amines for stabilizing Ag NPs on the tubes. To compare the catalytic efficacy of the MWCNT/Ag nanohybrid with silver oxide and silver nanoparticles, we calculated the turnover number (TON) and turnover frequency (TOF) for all three types of catalysts. Table 1 shows the data for the different systems.

Table 1: Catalytic efficiency of the MWCNT/Ag hybrid in comparison to the control systems.

Catalyst	Turnover number	Turnover frequency
silver(I) oxide	10.3	2.6 h^{-1}
silver(0) NPs	26.3	6.6 h^{-1}
Ag/MWCNT **1a**	33.3	8.3 h^{-1}

The catalyst based on CNTs is clearly more efficient in the conversion of the hydroquinone to benzoquinone than Ag_2O and Ag NPs alone. As shown in Table 1, the heterogeneous MWCNT/Ag catalysts feature the characteristics that are necessary for the reactions to run at higher rate in comparison to the silver oxide or metal nanoparticles. Moreover, the hybrid material can be easily recovered by simple filtration and can thus be immediately recycled. CNTs can be considered an efficient catalyst support because of their high specific surface area and chemical inertness. Our synthetic protocol proves that CNTs might become pliant materials by tuning their functionalization to promote the assembly of complex systems; this method is useful for the controlled and cost-effective design of new selective catalysts and for the production of advanced devices based on CNTs.

In conclusion, we have demonstrated the possibility to shape CNT functionalization in order to induce catalytic nanoparticle deposition. Adenine that is covalently bound to the CNT surface is able to trigger the formation of catalytic NPs with controlled sizes. This result provides the possibility for the tailored design of novel catalytic materials based on CNTs with full exploitation of their properties. Moreover, we have offered a proof-of-concept protocol by using this novel material as heterogeneous catalyst to promote the oxidation of hydroquinones, and by proving the catalytic efficiency of the nanohybrids on this model reaction and the complete recycling without loss of activity over multiple cycles.

Experimental Section

MWCNTs, produced by the catalytic carbon vapor deposition (CCVD) process, were purchased as purified from Nanocyl (thin MWCNT > 95% C purity, Nanocyl 3100 batch no. 071119), average diameter and length: 9.5 nm and 1.5 μm, respectively). Details of the synthesis of the ox-MWCNTs and the three Ad-MWCNTs **1a**, **1b**, and **1c** are reported in the Supporting Information.

Preparation of Ag NPs on Ad-MWCNTs **1a**, **1b**, and **1c**: 0.1 mg of the Ad-MWCNTs **1a**, **1b**, **1c**, ox-MWCNT, and f-MWCNT **9** (used as controls) were dispersed in methanol/water (1:1, 1 mL) by sonication for 5 min. A solution of $AgNO_3$ (1 or 5 equiv with respect to the adenine loading) in methanol/water (1:1, 1 mL) was prepared and added to the different functionalized carbon nanotubes. The resulting dispersions of **1a**, **1b**, **1c**, ox-MWCNT and f-MWCNT **9** were set aside for 10–12 h. After this period, some CNTs precipitated.

Catalysis: CNT-supported silver nanoparticles (1.00 mg of CNTs contain 0.0003 mmol of silver) and 35% aqueous hydrogen peroxide (4.0 μL, 0.05 mmol) were added to a solution of 2-methylhydroquinone (1.25 mg, 0.01 mmol) in methanol (0.50 mL). The resulting suspension was sonicated at room temperature until complete consumption of starting material and formation of 2-methylbenzoquinone was shown by HPLC. This analysis showed a selectivity of

> 99 % and a conversion of > 99 %. The silver/carbon nanotubes were recovered by centrifugation and recycled for successive catalytic cycles.

Received: April 29, 2011
Revised: July 29, 2011
Published online: September 14, 2011

Keywords: adenine · heterogeneous catalysis · nanoparticles · nanotubes · supramolecular chemistry

[1] *Carbon Nanotubes: Advanced Topics in the Synthesis, Structure, Properties and Applications* (Eds.: A. Jorio, G. Dresselhaus, M. S. Dresselhaus), Springer, Heidelberg, **2008**.
[2] M. T. Byrne, Y. K. Gun'ko, *Adv. Mater.* **2010**, *22*, 1672 – 1688.
[3] F. Cicoira, C. M. Aguirre, R. Martel, *ACS Nano* **2011**, *5*, 283 – 290.
[4] A. Le Goff, V. Artero, B. Jousselme, P. D. Tran, N. Guillet, R. Métayé, A. Fihri, S. Palacin, M. Fontecave, *Science* **2009**, *326*, 1384 – 1387.
[5] F. M. Toma, A. Sartorel, M. Iurlo, M. Carraro, P. Parisse, C. Maccato, S. Rapino, B. R. Gonzalez, H. Amenitsch, T. Da Ros, L. Casalis, A. Goldoni, M. Marcaccio, G. Scorrano, G. Scoles, F. Paolucci, M. Prato, M. Bonchio, *Nat. Chem.* **2010**, *2*, 826 – 831.
[6] P. Singh, S. Campidelli, S. Giordani, D. Bonifazi, A. Bianco, M. Prato, *Chem. Soc. Rev.* **2009**, *38*, 2214 – 2230.
[7] Special issue on carbon nanotubes, *Acc. Chem. Res.* **2002**, *35*, 997 – 1113.
[8] V. Georgakilas, D. Gournis, V. Tzitzios, L. Pasquato, D. M. Guldi, M. Prato, *J. Mater. Chem.* **2007**, *17*, 2679 – 2694.
[9] M. A. Correa-Duarte, L. M. Liz-Marzan, *J. Mater. Chem.* **2006**, *16*, 22 – 25.
[10] G. G. Wildgoose, C. E. Banks, R. G. Compton, *Small* **2006**, *2*, 182 – 193.
[11] A. T. Bell, *Science* **2003**, *299*, 1688 – 1691.
[12] D. R. Rolison, *Science* **2003**, *299*, 1698 – 1701.
[13] Q. Zhang, J. Xie, Y. Yu, J. Y. Lee, *Nanoscale* **2010**, *2*, 1962 – 1975.
[14] N. Karousis, N. Tagmatarchis, D. Tasis, *Chem. Rev.* **2010**, *110*, 5366 – 5397.
[15] B. Xue, P. Chen, Q. Hong, J. Lin, K. L. Tan, *J. Mater. Chem.* **2001**, *11*, 2378 – 2381.
[16] D. Wang, Z.-C. Li, L. Chen, *J. Am. Chem. Soc.* **2006**, *128*, 15078 – 15079.
[17] H. C. Choi, M. Shim, S. Bangsaruntip, H. Dai, *J. Am. Chem. Soc.* **2002**, *124*, 9058 – 9059.
[18] L. Qu, L. Dai, *J. Am. Chem. Soc.* **2005**, *127*, 10806 – 10807.
[19] B. M. Quinn, C. Dekker, S. G. Lemay, *J. Am. Chem. Soc.* **2005**, *127*, 6146 – 6147.
[20] T. M. Day, P. R. Unwin, N. R. Wilson, J. V. Macpherson, *J. Am. Chem. Soc.* **2005**, *127*, 10639 – 10647.
[21] G.-P. Jin, R. Baron, N. V. Rees, L. Xiao, R. G. Compton, *New J. Chem.* **2009**, *33*, 107 – 111.
[22] C. Burda, X. Chen, R. Narayanan, M. A. El-Sayed, *Chem. Rev.* **2005**, *105*, 1025 – 1102.
[23] Y. Lin, K. A. Watson, M. J. Fallbach, S. Ghose, J. G., Jr. Smith, D. M. Delozier, W. Cao, R. E. Crooks, J. W. Conell, *ACS Nano* **2009**, *3*, 871 – 884.
[24] A. B. Castle, E. E. Gracia-Espino, C. Nieto-Delgado, H. Terrones, M. Terrones, S. Hussain, *ACS Nano* **2011**, *5*, 2458 – 2466.
[25] *The Chemistry of Quinonoid Compounds*, *Vol. 1 – 2*, Part 1 (Ed.: S. Patai), Wiley, New York, **1988**.
[26] S. Verma, A. K. Mishra, J. Kumar, *Acc. Chem. Res.* **2010**, *43*, 79 – 91.
[27] E. Fortunati, F. D'Angelo, S. Martino, A. Orlacchio, J. M. Kenny, I. Armentano, *Carbon* **2011**, *49*, 2370 – 2379.
[28] L. H. Tjeng, B. M. J. Meinders, J. Van Elp, J. Ghijsen, G. A. Sawatzky, R. L. Johnson, *Phys. Rev. B* **1990**, *41*, 3190 – 3199.
[29] NIST Standard Reference Database 71, version 1.1.
[30] C. Gao, W. Li, Y. J. Zheng, H. Kong, *Nanotechnology* **2006**, *17*, 2882 – 2891.
[31] S. Ayyappan, R. S. Gopalan, G. N. Subbanna, C. N. R. Rao, *J. Mater. Res.* **1997**, *12*, 398 – 401.
[32] I. Brehm, S. Hinneschiedt, H. Meier, *Eur. J. Org. Chem.* **2002**, 3162 – 3170.
[33] L. Alaerts, J. Wahlen, P. A. Jacobs, D. E. De Vos, *Chem. Commun.* **2008**, 1727 – 1737.
[34] O. V. Zalomaeva, O. A. Kholdeeva, A. B. Sorokin, *Green Chem.* **2006**, *8*, 883 – 886.
[35] F. Derikvand, F. Bigi, R. Maggi, C. G. Piscopo, G. Sartori, *J. Catal.* **2010**, *271*, 99 – 103.
[36] *Oxidative Coupling of Phenols* (Eds.: W. I. Taylor, A. R. Battersby), M. Dekker, New York, **1967**.